

# DECORATION OF CYCLODEXTRIN ON SURFACE OF POROUS NANOSILICA VIA DISULFIDE BOND FOR THE CONTROLLED DRUG RELEASE

Dai Hai Nguyen<sup>1,2,\*</sup>, Thai Thanh Hoang Thi<sup>2,3</sup>

<sup>1</sup>Graduate University of Science and Technology, VAST, 18 Hoang Quoc Viet, Cau Giay, Ha Noi, Viet Nam

<sup>2</sup>Institute of Applied Materials Science, VAST, 1 TL29, Dis. 12, Ho Chi Minh City, Viet Nam

<sup>3</sup>Biomaterials and Nanotechnology Research Group, Faculty of Applied Sciences, Ton Duc Thang University, Ho Chi Minh City, Viet Nam

\*Email: [nguyendaihai@iams.vast.vn](mailto:nguyendaihai@iams.vast.vn)

Received: 4 February 2020; Accepted for publication: 28 June 2020

**Abstract.** Porous nanosilica (PNS) as promising targeted drug nanocarriers has become a new area of interest in recent years due to their tunable pore sizes and large pore volumes, high chemical and thermal stability, and excellent biocompatibility. These unique structures of PNS facilitate effective protecting drugs from degradation and denaturation. However, it has certain limitations for being used in pharmaceutical such as a burst release of encapsulated drugs. In this study, the effects of grafting cyclodextrin (CD) as gatekeeper through the biodegradable disulfide bonds on doxorubicin (DOX) release was investigated. The morphology and pore channel structures of these modified PNS were assessed by transmission electron microscopy (TEM). Fourier transform infrared spectroscopy (FTIR) was utilized to evaluate the functional groups on PNS surface. *In vitro* tests were conducted for the drug loading and releasing efficiency. The results demonstrated that the prepared DOX@PNS-SS-A/CD was of spherical shape with an average diameter of 45 nm, drug loading efficiency of  $60.52 \pm 2.12$  %, and sustained release. More importantly, MTT assay showed that PNS-SS-A/CD was biocompatible nanocarriers. In addition, the modified PNS incorporating DOX could significantly eliminate the toxicity of free DOX. As a result, the development of PNS-SS-A/CD may offer a promising candidate for loading and sustained release of DOX in cancer therapy.

**Keywords:** drug delivery system, porous nanosilica, cyclodextrin, doxorubicin.

**Classification numbers:** 2.2.4, 2.5.3, 2.7.1.

## 1. INTRODUCTION

During the last three decades, porous nanosilica (PNS) has emerged as a promising targeted drug nanocarrier due to the unique porous structure, chemical and thermal stabilities, biocompatibility, biodegradability, and surface functionality that ensures the controlled release of a variety of anticancer drugs [1 - 4]. The porous architecture of PNS allows loading a large

number of drugs inside the pores and protecting them from degradation as well as denaturation [5]. However, the encapsulated drug in bare PNS could not overcome the burst release phenomenon that is one major drawback needed to be surpassed by other techniques [6, 7]. Thus, many different methods functionalizing the PNS surface have been developed. Nevertheless, several studies demonstrated that such conditions can control and delay the rate of drug release.

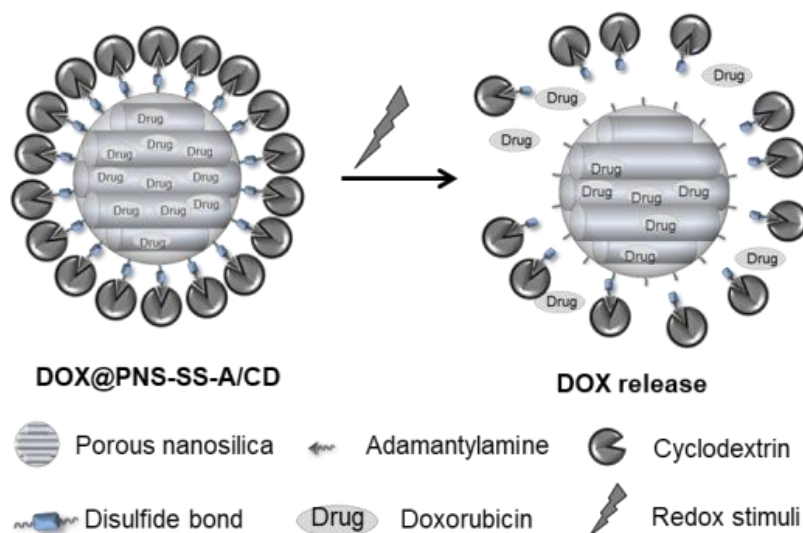


Figure 1. Schematic illustration showing the formation and redox-sensitive intracellular delivery of DOX-loaded PNS-SS-A/CD nanoparticles.

Stimuli-responsive PNS has been developed to induce the controlled drug release triggered by temperature, light, pH, redox potential, magnetic, electric and mechanical stimuli, as well as enzyme and chemical reactions [8, 9]. Among different types of stimuli-responsive PNSs, redox stimulus is competitive PNS for loading drugs in the pores because it takes advantage of intracellular conditions, namely the presence of glutathione (GSH) in tumor cells that is approximately three times higher than that in normal cells. Moreover, GSH in tumor cell leads to cleave redox-groups and trigger the delivery of therapeutic agents [10]. Therefore, stimuli-responsive PNSs which have disulfide bonds (S–S) as redox-sensitive groups and disulfide-linked cyclodextrin (CD) as gatekeepers could be easily cleaved in the presence of GSH which makes it an attracting redox-responsive system to release drugs at the targeted tumor sites [11 - 13]. The structure of PNS delivery systems, in particular, was modified to be capable of encapsulating a variety of therapeutic agents at exceptionally high loadings [14]. For instance, Abdous *et al.* reported the redox-responsive drug delivery system using  $\beta$ -Cyclodextrin to block the pore entrances of PNS through a biodegradable disulfide bond to achieve controlled release of curcumin (CUR) [15]. The results showed that the maximum loading efficiency was 88.55% at 43 h of loading time and 1.22 % of the weight ratio. The maximum CUR release was obtained at 5.16 of pH and 107 h of release time. This novel [ $\beta$ -CD@PEGylated KIT-6] nanoparticles exhibited stimuli-responsive drug release property and can be further used as a promising candidate for cancer treatment [15].

Herein, we report on the redox-controlled release of Doxorubicin (DOX) entrapped in the pore of PNS that is blocked by the surface-grafted redox-responsive SS-A/CD. The mechanism of this system is schematically described in Figure 1. The modified PNS was characterized using

different techniques such as Fourier transform infrared (FTIR) and transmission electron microscope (TEM). The drug releasing behavior of the prepared DOX@PNS-SS-A/CD was also determined using dithiothreitol (DTT) which was used to reduce –SS– in PNS-SS-A/CD. Additionally, MTT assay was performed to determine whether the PNS-SS-A/CD may reduce the toxicity to HeLa cells of DOX. The aim of this study is to create an efficiency redox-sensitive PNS for controlled drug delivery.

## 2. MATERIALS AND METHODS

### 2.1. Materials

Ethanol absolute (EtOH, 46.07 g/mol), toluene was purchased from Scharlab, Spain. Tetraethyl orthosilicate 98 % (TEOS, 208.33 g/mol), N,N-dimethyl formamide (DMF, 73.09 g/mol), dithiothreitol (DTT, 154.25 g/mol), ethylenediamine (EDA, 60.10 g/mol), 1-ethyl-3-(3-dimethylaminopropyl) carbodimide (EDC, 191.70 g/mol), amantadine hydrochloride (A, 187.71 g/mol), and doxorubicin (DOX, 579.98 g/mol) were obtained from Sigma-Aldrich, USA. N-cetyl-nnn-trimethylammonium bromide (CTAB, 364.45 g/mol), acetone nitrile (ACN, 41.05 g/mol) were purchased from Merck, Germany.  $\beta$ -cyclodextrin ( $\beta$ -CD, 1134.99 g/mol) was purchased from TCI, Japan. 3,3'-dithiodipropionic acid (DTDP) 99 % (210.26 g/mol) and (3-aminopropyl)triethoxysilane (APS) 99 % (221.37 g/mol) were purchased from Acros Organics, Belgium. All chemicals were of ACS reagent grade and used without further purification.

### 2.2. Synthesis of PNS-SS-A and PNS-SS-A/CD

Based on the literature with minor modification, the overall PNS-SS-A synthesis can be described in four steps [2]. First, PNS was synthesized by the sol-gel process including TEOS as alkoxide precursors, CTAB as surfactant, ethanol/water/ammonia solution ( $\text{NH}_3$ ) as a solvent. Deionized water ( $\text{deH}_2\text{O}$ , 64 mL), ethanol (11.25 mL, 0.2 mol), CTAB (2.6 g, 7.1 mmol), and 2.8 %  $\text{NH}_3$  solution (0.55 mL, 0.9 mmol) were mixed at 60 °C with a stir-bar for 30 min. TEOS (8 mL, 35.8 mmol) were added drop-wise to the surfactant solution within 5 min under stirring for 2 h, and then filtered. The filtrated solution was dialyzed using a dialysis membrane (MWCO 6-8 kDa, Spectrum Laboratories, Inc., USA) against  $\text{deH}_2\text{O}$  for 4 days at room temperature. The  $\text{deH}_2\text{O}$  was changed 5-6 times per day. The dialyzed mixture was then lyophilized to obtain PNS. Secondly, the amine functionalized PNS (PNS- $\text{NH}_2$ ) were prepared by the interaction between APS (1 mL, 5.7 mmol) and PNS (1 g) in toluene (30 mL). The reaction was performed at room temperature under stirring and nitrogen conditions for 24 h. The suspension was dialyzed using a dialysis membrane (MWCO 6-8 kDa) for 4 days against 2 M of acetic acid:ethanol (1:1 v/v, 250 mL). Acetic acid:ethanol solution was changed 5-6 times per day, and then the tube containing PNS was immersed into  $\text{deH}_2\text{O}$  to remove acetic acid/EtOH for 1 day. The  $\text{deH}_2\text{O}$  was changed 5-6 times a day and the resulting solution was lyophilized to generate PNS- $\text{NH}_2$  as white powder. Thirdly, the conjugation of the disulfide bond onto PNS- $\text{NH}_2$  was carried out by the reaction between PNS- $\text{NH}_2$  and DTDP to form PNS-SS-COOH. In brief, the obtained PNS- $\text{NH}_2$  (1 g) and EDC (0.14 mL, 0.77 mmol) were dissolved in  $\text{deH}_2\text{O}$  (20 mL) under stirring for 10 min. Then, DTDP (0.16 g, 0.77 mmol) in DMF (20 mL) were added into the mixture and the reaction was maintained for 24 h. After that, the sample was purified by a dialysis membrane (MWCO 6-8 kDa) against  $\text{deH}_2\text{O}$  at room temperature for 4 days. This purified solution was lyophilized to obtain PNS-SS-COOH. Finally, the adamantane conjugated PNS-SS-COOH (named as PNS-SS-A) was synthesized. The reaction including PNS-SS-COOH

(1 g), a solution (0.77 mmol) and EDC (0.64 mmol) was stirred at room temperature for 24 h. After completing reaction, the mixture was filtered and then dialyzed for 4 days. The deH<sub>2</sub>O was changed 5-6 times per day. The mixture after dialysis was lyophilized to obtain PNS-SS-A.

To prepare PNS-SS-A/CD, 200 mg of PNS-SS-A was immersed in 40 ml of deionized water and then mixed with 44 mg of  $\beta$ -CD. The sample was dialyzed in a cellulose tube (MW 12000-14000 Da) for 4 days with the water changing of 4 times/day. The lyophilization was done to obtain PNS-SS-A.

### **2.3. Characterization**

Morphology and size of the resulting PNS were observed with a TEM (JEM-1400, JEOL, Tokyo, Japan). The accelerating voltage was operated at 200 kV. The copper formvar/carbon grids were utilized. The samples were dispended and sonicated in ethanol. Dropping the samples on the grids, they were dried for 24 hours before measuring.

FTIR spectra were performed (Nicolet 5700, Thermo Electron Corporation, MA, USA) in the transmittance mode at the wavenumber range of 4000 - 500 cm<sup>-1</sup> to evaluate the functional groups on silica surface. The PNS, PNS-SS-A and PNS-SS-A/CD were mixed in potassium bromide salt, then pressed into the thin pellet which would be scanned by FTIR spectrophotometer.

The samples were outgassed at 150 °C for 3 h, then nitrogen adsorption-desorption isotherms were determined by NOVA 1000e system (Quantachrome Instruments, USA).

X-ray diffraction measurements (Rigaku DMAX 2200PC, Rigaku Americas Co., USA) were performed to identify the phase of materials. The diffractometer was equipped with Cu/K $\alpha$  radiation ( $\lambda = 0.15405$  nm), the scanning rate was 4°/min.

### **2.4. Drug loading**

The model drug DOX was used in drug loading and drug releasing study. Typically, 100 mg PNS-SS-A were immersed in 20 ml of DOX solution in deionized water (0.2 mg/ml). After stirring for 24 hours under dark conditions, the DOX loaded nanoparticles were dialyzed in 5 hours to remove excessive DOX. The  $\beta$ -CD (22 mg) was used to seal the loading nanoparticles [16]. The product was obtained as DOX@PNS-SS-A/CD. Similarly, the unmodified PNS loading DOX (DOX@PNS) was prepared for control group. The particles were used for subsequent tests of DOX release. DOX loaded inside the nanoparticles was determined by UV absorption at 541 nm. The obtained particles were freeze-dried prepared for controlled release experiments. These experiments were repeated 3 times and the results were a mean of time determination.

### **2.5. Drug released behavior**

The drug released study was performed by the introduction of reducing agent DTT. The DTT triggered release of DOX from two different DOX@PNS-SS-A/CD samples were obtained by dialysis method with cellulose dialysis membrane (MW = 12000-14000 Da). The released buffer to stimulate body fluid environment contained PBS buffer (pH 7.4, 0.01 M) and DTT (5 mM) as external stimulus to breakdown disulfide linkage. The DOX release profile was calculated by measuring the absorbance of the released DOX solution at wavelength 541 nm using UV-Vis spectroscopy.

## 2.6. Cell study

To evaluate the effect of DOX loaded PNS-SS-A/CD on killing cancerous cells in the comparison with CD, PNS-SS-A/CD and free DOX, HeLa cell lines were used. HeLa cells were cultured on 96-well plates for 1 days with  $1.5 \times 10^4$  cells/well. Then they were washed with DPBS for three times. The cell media (DMEM mixing with 10 % of FBS and 1 % of PS) were mixed with CD, PNS-SS-A/CD (100  $\mu\text{g/mL}$ ), free DOX, and DOX loaded PNS-SS-A/CD (eq. DOX concentration of 5  $\mu\text{g/mL}$ ) to add respectively into each HeLa cell well. Each sample was repeated three times. All cells were kept for 72 hours in an incubator at 37 °C, relative humidity of 98 % and CO<sub>2</sub> of 5 %. After each 24-hour contacting those materials, the cells were characterized of the viability using resazurin test method. To measure the viability, the media was removed and added 10  $\mu\text{L}$  of resazurin solution (0.2 mg/mL). The well-plates were kept to be reacted for 4 hours. Then 100  $\mu\text{L}$  of cell media of each well was moved into 96-well plate to read with microplate reader at excitation/emission of 560/590 nm.

## 3. RESULTS AND DISCUSSION

### 3.1. Characteristics

The morphology and pore channel structures of prepared particles were analyzed with TEM. The white products highly and stably suspended in solution with centrosymmetric radial mesopores. The bare PNS and modified PNS (PNS-SS-A/CD) were in the diameter range of 40-50 nm (Figure 2a, b). The size and shape of PNS and modified PNS were comparable, so the nanoparticles could keep their morphology after the functionalization. This synthesized PNS diameter was almost similar with mesoporous nanosilica of Menard *et al.* [17] However, the PNS-SS-A/CD diameter was significantly smaller than other modified PNS. For example, the poly(acrylic acid) functionalized mesoporous silica nanoparticles were 180 nm [18], the aminopropyl modified nanoporous silica nanoparticles designed by Wang *et al.* were 100 - 130 nm [19]. Al-Nadaf *et al.* utilized polyethylene glycol or polypropylene glycol to wrap mesoporous silica nanoparticles and obtained the modified MSNs of 357 or 580 nm [20]. It could be reasoned that the polymers with long chains enlarged the MSN size, while our study utilized the small molecules not causing any change much in nanoparticle dimension. However, the mesopore arrays couldn't be clearly observed in aqueous solution, because of the polymer envelope (Figure 2b).

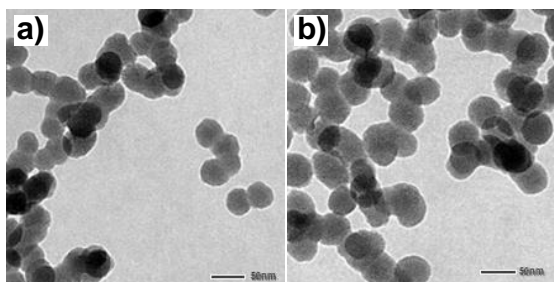


Figure 2. TEM images of prepared PNS (a) and PNS-SS-A/CD (b).

The surface modification of PNS was determined by FTIR. In Figure 3, three FTIR spectra showed the peak of 1092  $\text{cm}^{-1}$  was assigned to asymmetric stretching of Si-O-Si bond in the

silica nanoparticles [21]. After grafting amantadine on the nanoparticle surface to form PNS-SS-A, a new peak appeared at  $1530\text{ cm}^{-1}$  attributed to the primary amine groups (Figure 3b). In addition, the peaks of  $2930$  and  $2860\text{ cm}^{-1}$  assigned to C-H stretching vibration were also observed in PNS-SS-A spectra. The broad peak from  $1100$  to  $1300\text{ cm}^{-1}$  overlapped the signals for the A units on the nanoparticle surface [22]. These FTIR results indicated that the amantadine was conjugated successfully onto MSN surface. In the Figure 3c, a peak at  $\sim 1643\text{ cm}^{-1}$  corresponding to the H-O-H bending of  $\beta$ -CD structure [23] that implied the  $\beta$ -CD-capped PNS-SS-A.

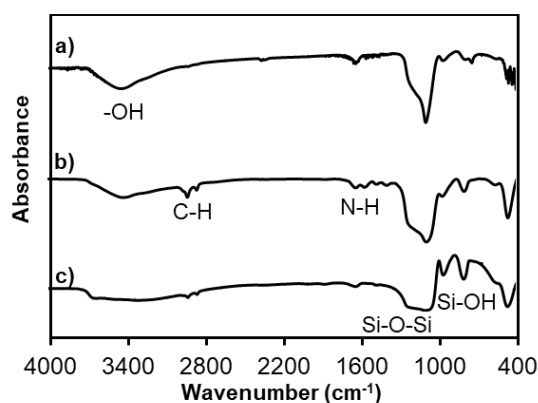


Figure 3. FTIR spectra of PNS (a), PNS-SS-A (b), PNS-SS-A/CD (c).

To determine the crystalline species of mesoporous silica structures, XRD was carried out. Figure 4 showed the measured XRD pattern of PNS and PNS-SS-A/CD. In two XRD spectra of bare PNS (Figure 4a) and modified PNS-SS-A/CD (Figure 4b), the broad band of 2 $\theta$  degree was observed that was assigned as the characteristic diffraction peak due to (100), (110) and (200) planes of amorphous silica nanosphere [24]. However, the diffraction intensity of PNS-SS-A/CD seemed smaller than that of bare PNS. This could be ascribed to the presence of organic moiety amount in PNS-SS-A/CD. Altogether, the modification of cyclodextrin and amantadine on PNS surface did not change the amorphous phase of PNS.

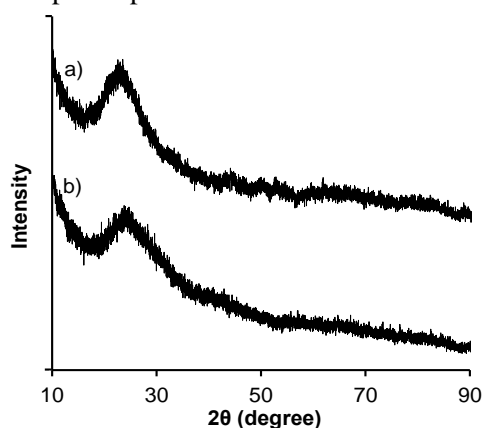


Figure 4. XRD patterns of PNS (a) and PNS-SS-A/CD (b).

To characterize the porous materials,  $\text{N}_2$  adsorption-desorption method is considered as a well-established technique. Figure 5 showed the nitrogen adsorption-desorption isotherm of

PNS-SS-A/CD nanoparticles. Following the IUPAC classification, this isotherm was belonging to the IV(a) type associated with adsorption in mesoporous materials containing 2-50 nm of pore width. The lower relative pressures ( $P/P_0$ ,  $P_0$  was saturation pressure of adsorption) were applied to the smaller volume, vice versa, the higher  $P/P_0$  was used for the larger volume. At 417.56  $\text{cm}^3/\text{g}$  of PNS-SS-A/CD, the pressure was plateau, the pore volume of PNS-SS-A/CD was determined. As our previous study, the pore volume of bare PNS was reported as 710.40  $\text{cm}^3/\text{g}$ . So the functionalization of PNS using adamantine and  $\beta$ -CD caused the reduction on the pore volume of silica nanoparticles. Moreover, the hysteresis loop at  $P/P_0$  range of 0.38 - 0.98 was appeared in this isotherm. This feature was associated with the metastability of the mesoporous adsorption. Taken together, the porous structure of silica nanoparticles were retained well after modifying with adamantine and  $\beta$ -CD.

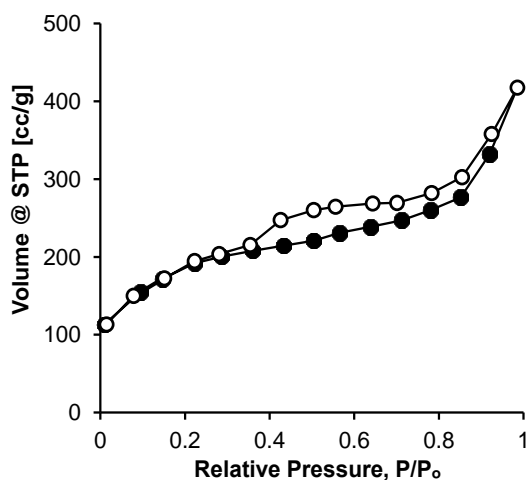


Figure 5. Nitrogen adsorption–desorption isotherm of PNS-SS-A/CD.

### 3.2. Drug loading

To demonstrate the drug carrier ability of PNS and modified-PNS, DOX was encapsulated inside these systems and their loading efficiency was tested. The loading efficiencies of DOX in PNS and CD modified-PNS were  $19.59 \pm 2.14 \%$  and  $60.52 \pm 2.12 \%$ , respectively. The major obstacle of unmodified surface silica nanoparticles was the low loading efficiency, drug molecules would start leaking out of the particles intermediately when they were introduced in water so PNS exhibited a little bit lower DOX loading capacity than modified-PNS. The gatekeeper system and CD end-capped illustrated the efficiency in increasing drug loading level. Also the loading efficiency of PNS-SS-A/CD (60.52 %) was comparable to other similar studies. Guo *et al.* formed the  $\beta$ -CD-poly(N-isopropylacrylamide)@mesoporous silica-ferrocene with doxorubicin loading efficiency of 66.68 - 71.04 % [25]. In addition, Gupta *et al.* reported the hyaluronic acid-capped mesoporous titania nanoparticles with doxorubicin loading capacity of 18.3 % [26]. Xin *et al.* reported the amino modified multimodal nanoporous silica nanoparticles with loading capacity of 34.52 % [19]. Despite of various drug loading efficiency/capacity, each system achieved its own outstanding properties and showed excellent effect on killing cancerous cells.

### 3.3. Evaluation of drug release behavior

The released amount of DOX was calculated based on the measurement of DOX calculated from the standard curve. As seen in Figure 6 (black column), the rapid release of DOX in DOX@PNS system was observed because the matrix-entrapped drug would start leaking out the biodegradable carrier right after the system was introduced in aqueous solution. However, the DOX@PNS system could slow down the DOX release compared to free DOX due to the hindrance space. The DOX@PNS-SS-A/CD showed the lowest amount of released DOX due to the highest hindrance caused by both porous silica and the capping CD. In case of using the media containing DTT, the release profile in two different media could exhibit the significant change only for DOX@PNS-SS-A/CD system. In fact, as showed in Figure 6 (white column), the released DOX amount in DTT media was two-fold higher than that in PBS for DOX@PNS-SS-A/CD, while there was no change observed for free DOX and DOX@PNS-SS-A. This phenomenon indicated the important role of CD capped outside the porous nanosilica particles. The capping CD was not only to limit the DOX release in normal condition but also to enhance the DOX release rate in the DTT solution as reducing agents. These results implied that DOX@PNS-SS-A/CD could limit the free DOX leak out in the normal tissues, but induce the burst release in cancerous organs due to high level of glutathione being a reducing agent. Thus, the DOX@PNS-SS-A/CD being glutathione-sensitive system was successfully designed to cause burst release in cancer cells to increase the killing effect, while less leakage was occurred in the normal cell conditions. Looking at another strategies, sulfonate-functionalized doxorubicin-loaded mesoporous silica nanoparticles exploited the presence of serum to enhance the drug loading and to accelerate their release ability, almost 50 % of doxorubicin were released after 6 hours [27]. Gupta *et al.* exploited hyaluronic acid as targeting agent of CD44 on cancer cell to fabricate the doxorubicin release system, they also achieved over 60 % doxorubicin going out after 24 hours [26]. Although each strategy obtained the various release profile, all showed the good effect on killing cancer cells.

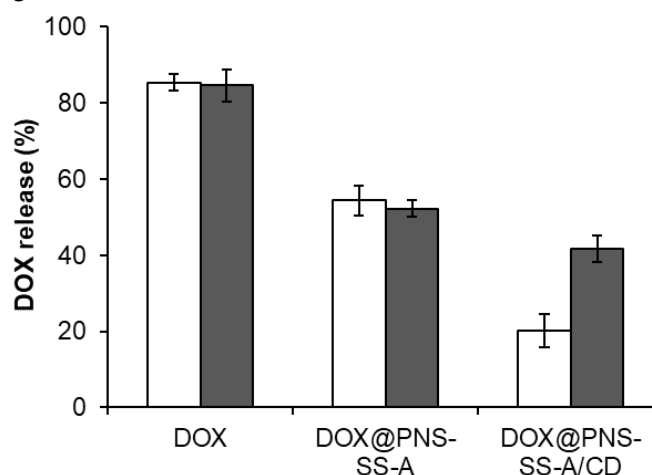


Figure 6. Percentage of release of DOX, DOX@PNS-SS-A and DOX@PNS-SS-A/CD in pH 7.4 PBS with (white column) and without DTT (5 mM, black column) at 24 h.

### 3.4. *In vitro* cytotoxicity

The *in vitro* cytotoxicity effect of the  $\beta$ -CD, PNS-SS-A/CD, DOX@PNS-SS-A/CD, and free DOX against Hela cells was determined. Figure 7 described the Hela cell viability when they were incubated with four aforementioned samples. In  $\beta$ -CD and PNS-SS-A/CD media, Hela cells were grown up normally, 100 % viability compared to fresh media is an acceptable



value for non-cytotoxicity. This data confirmed that these materials did not cause any effect on HeLa cells. In case of DOX@PNS-SS-A/CD test, HeLa cell viability was significantly decreased to 70 % after 24-hour incubation, and continuously down to 55 % and 20 % after 48 and 72 hour. Taken together, the killing effect was caused by released DOX. In addition, the decreased viability of HeLa cells contacting DOX@PNS-SS-A/CD was comparable to that of free DOX that implied the DOX@PNS-SS-A/CD system did not compromise the efficiency of free DOX in killing cancerous cells. These results confirmed the promising application of PNS-SS-A/CD with controlled drug delivery and highly killing effect being comparable to free drug.

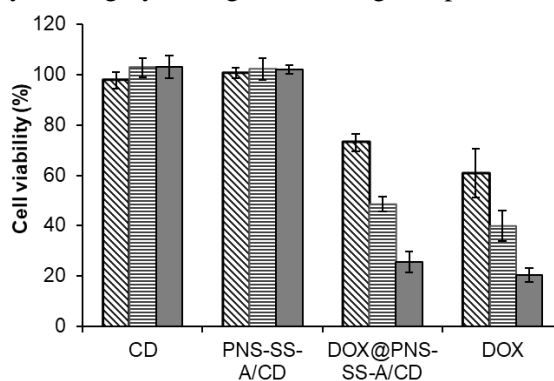


*Figure 7.* Viability of HeLa cells incubated with CD, PNS-SS-A/CD (100  $\mu\text{g}/\text{mL}$ ), free DOX, and DOX loaded PNS-SS-A/CD (eq. DOX concentration of 5  $\mu\text{g}/\text{mL}$ ) for 24, 48 and 72 h, respectively. The cells were exposed to the samples for the indicated times. The data represent the mean values  $\pm$  the standard deviation (SD) (n = 4).

#### 4. CONCLUSIONS

The  $\beta$ -CD functionalized porous nanosilica through disulfide linkages has been successfully prepared. The introduction of disulfide in drug delivery system was to offer the redox-responsive mechanism, the capping  $\beta$ -CD was utilized with a function of gatekeeper. In cancerous cells, the disulfide linkage can be effectively cleaved by antioxidant agents, resulting in the detachment of  $\beta$ -CD to open the door of porous nanosilica particles for the burst release of drug. Specifically, the size of DOX@PNS-SS-A/CD was less than 100 nm that is suitable for penetrating inside the cells. The loading efficiency was highly  $60.52 \pm 2.12$  %. The release rate of DOX@PNS-SS-A/CD was controlled and induced by a reducing agent. Therefore, the DOX@PNS-SS-A/CD exhibited its ability as a promising candidate for drug delivery system with stimuli response.

**Acknowledgements.** This research was funded by Vietnam National Foundation for Science and Technology Development (NAFOSTED) under grant no. 104.03-2018.46.

#### REFERENCES

1. Kong D., Pan H., Wang L., Corr D. J., Yang Y., Shah S. P., Sheng J. - Effect and mechanism of colloidal silica sol on properties and microstructure of the hardened cement-based materials as compared to nano-silica powder with agglomerates in micron-scale, *Cement and Concrete Composites* **98** (2019) 137-149.

2. Nguyen A. K., Nguyen T. H., Bao B. Q., Bach L. G., Nguyen D. H. - Efficient self-assembly of mPEG end-capped porous silica as a redox-sensitive nanocarrier for controlled doxorubicin delivery, *International Journal of biomaterials* **2018** (2018) 1575438.
3. Ho M. N., Bach L. G., Nguyen D. H., Nguyen C. H., Nguyen C. K., Tran N. Q., Nguyen N. V., Hoang Thi T. T. - PEGylated PAMAM dendrimers loading oxaliplatin with prolonged release and high payload without burst effect, *Biopolymers* **110** (7) (2019) e23272.
4. Nguyen Le M. T., Nguyen D. T. D., Rich S., Nguyen N. T., Nguyen C. K., Nguyen D. H. - Synthesis and characterization of silica coated magnetic iron oxide nanoparticles, *Vietnam Journal of Science and Technology* **57** (3A) (2019) 160.
5. Bao B. Q., Le N. H., Nguyen D. H. T., Tran T. V., Pham L. P. T., Bach L. G., Ho H. M., Nguyen T. H., Nguyen D. H. - Evolution and present scenario of multifunctionalized mesoporous nanosilica platform: A mini review, *Materials Science and Engineering: C* **91** (2018) 912-928.
6. Zhang B., Tan H., Shen W., Xu G., Ma B., Ji X. - Nano-silica and silica fume modified cement mortar used as Surface Protection Material to enhance the impermeability, *Cement and Concrete Composites* (2018) 7-17.
7. Thi N. T. N., Nguyen D. H. - Hollow mesoporous silica nanoparticles fabrication for anticancer drug delivery, *Vietnam Journal of Science and Technology* **58** (1) (2020) 39.
8. Thi T. T. H., Nguyen T. N. Q., Hoang D. T., Ngo V. C., Nguyen D. H. - Functionalized mesoporous silica nanoparticles and biomedical applications, *Materials Science and Engineering: C* **99** (2019) 631-656.
9. Vo U. V., Nguyen C. K., Nguyen V. C., Tran T. V., Thi B. Y. T., Nguyen D. H. - Gelatin-poly (ethylene glycol) methyl ether-functionalized porous Nanosilica for efficient doxorubicin delivery, *Journal of Polymer Research* **26** (2019) 6.
10. Thi T. T. N., Tran T. V., Tran N. Q., Nguyen C. K., Nguyen D. H. - Hierarchical self-assembly of heparin-PEG end-capped porous silica as a redox sensitive nanocarrier for doxorubicin delivery, *Materials Science and Engineering: C* **70** (2017) 947-954.
11. Thi N. T. N., Le N. H., Vo U. V., Nguyen C. K., Nguyen D. H. - Engineering of Hollow Mesoporous Silica Nanoparticles Enhancing Drug-Loading Capacity, In *Proceedings of International Conference on the Development of Biomedical Engineering in Vietnam* **69** (2018) 197-201.
12. Nguyen D. H. T., Nguyen D. Y. P., Pham L. P. T., Vo T. N. N., Nguyen D. H., Park K. D. - Preparation and Characterization of Redox-Sensitive Pluronic F127-Based Nanogel as Effective Nanocarrier for Drug Delivery, In *Proceedings of International Conference on the Development of Biomedical Engineering in Vietnam* **69** (2018) 189-192.
13. Nguyen D. H. - Design and decoration of heparin on porous nanosilica via reversible disulfide linkages for controlled drug release, *Journal of the Institute of Korean Electrical and Electronics Engineers* **21** (2017) 320-330.
14. Tran T. V., Vo U. V., Pham D. Y., Nguyen T. H., Tran N. Q., Nguyen C. K., Nguyen D. H. - Supramolecular chemistry at interfaces: Host-guest interactions for attaching PEG and 5-fluorouracil to the surface of porous nanosilica, *Green Processing and Synthesis* **5** (6) (2016) 521-528.
15. Abdous B., Sajjadi S. M., Ma'mani L.-  $\beta$ -Cyclodextrin modified mesoporous silica nanoparticles as a nano-carrier: response surface methodology to investigate and optimize

- loading and release processes for curcumin delivery, *Journal of Applied Biomedicine* **15** (3) (2017) 210-218.
16. Dai L., Li J., Zhang B., Liu J., Luo Z., Cai K. - Redox-responsive nanocarrier based on heparin end-capped mesoporous silica nanoparticles for targeted tumor therapy *in vitro* and *in vivo*, *Langmuir* **30** (26) (2014) 7867-7877.
  17. Menard M., Meyer F., Parkhomenko K., Leuvrey C., Francius G., Begin-Colin S., Mertz D. - Mesoporous silica templated-albumin nanoparticles with high doxorubicin payload for drug delivery assessed with a 3-D tumor cell model, *Biochim Biophys Acta Gen Subj.* **1863** (2) (2019) 332-341.
  18. Li H., Zhang J. Z., Tang Q., Du M., Hu J., Yang D. - Reduction-responsive drug delivery based on mesoporous silica nanoparticle core with crosslinked poly(acrylic acid) shell, *Materials Science and Engineering: C* **33** (6) (2013) 3426-3431.
  19. Wang X., Li C., Fan N., Li J., He Z., Sun J. - Multimodal nanoporous silica nanoparticles functionalized with aminopropyl groups for improving loading and controlled release of doxorubicin hydrochloride, *Materials Science and Engineering: C* **78** (2017) 370-375.
  20. Al-Nadaf A. H., Dahabiyeh L. A., Bardaweel S., Mahmoud N. N., Jawarneh S. - Functionalized mesoporous silica nanoparticles by lactose and hydrophilic polymer as a hepatocellular carcinoma drug delivery system, *Journal of Drug Delivery Science and Technology* **56** (2020) 101504.
  21. Wang T. T., Lan J., Zhang Y., Wu Z. L., Li C. M., Wang J., Huang C. Z. - Reduced graphene oxide gated mesoporous silica nanoparticles as a versatile chemo-photothermal therapy system through pH controllable release, *Journal of Materials Chemistry B* **3** (30) (2015) 6377-6384.
  22. Ma X., Teh C., Zhang Q., Borah P., Choong C., Korzh V., Zhao Y. - Redox-responsive mesoporous silica nanoparticles: a physiologically sensitive codelivery vehicle for siRNA and doxorubicin, *Antioxidants and redox signaling* **21** (5) (2014) 707-722.
  23. Menezes P. P., Serafini M. R., Santana B. V., Nunes R. S., Quintans Jr L. J., Silva G. F., Medeiros I. A., Marchioro M., Fraga B. P., Santos M. R. - Solid-state  $\beta$ -cyclodextrin complexes containing geraniol, *Thermochimica Acta* **548** (2012) 45-50.
  24. Bardhan M., Majumdar A., Jana S., Ghosh T., Pal U., Swarnakar S., Senapati D. - Mesoporous silica for drug delivery: Interactions with model fluorescent lipid vesicles and live cells, *Journal of Photochemistry and Photobiology B: Biology* **178** (2018) 19-26.
  25. Guo F., Li G., Zhou H., Ma S., Guo L., Liu X. - Temperature and H<sub>2</sub>O<sub>2</sub>-operated nano-valves on mesoporous silica nanoparticles for controlled drug release and kinetics. *Colloids and surfaces, B Biointerfaces* **187** (2020) 110643.
  26. Gupta B., Poudel B. K., Ruttala H. B., Regmi S., Pathak S., Gautam M., Jin S. G., Jeong J. H., Choi H. G., Ku S. K., et al. - Hyaluronic acid-capped compact silica-supported mesoporous titania nanoparticles for ligand-directed delivery of doxorubicin, *Acta biomaterialia* **80** (2018) 364-377.
  27. Shahabi S., Doscher S., Bollhorst T., Treccani L., Maas M., Dringen R., Rezwani K. - Enhancing Cellular Uptake and Doxorubicin Delivery of Mesoporous Silica Nanoparticles via Surface Functionalization: Effects of Serum, *ACS applied materials and interfaces* **7** (48) (2015) 26880-26891.